

Linear Theory of Electron-Plasma Waves at Arbitrary Collisionality

R. Jorge^{1,2,†‡}, P. Ricci¹, S. Brunner¹, S. Gamba^{1,3}, V. Konovets¹, N. F. Loureiro⁴, L. M. Perrone¹, and N. Teixeira²

¹École Polytechnique Fédérale de Lausanne (EPFL), Swiss Plasma Center (SPC), CH-1015 Lausanne, Switzerland

²Instituto de Plasmas e Fusão Nuclear, Instituto Superior Técnico, Universidade de Lisboa, 1049-001 Lisboa, Portugal

³Department of Energy, Politecnico di Milano, Via Ponzio 34/3, Milano, 20133, Italy

⁴Plasma Science and Fusion Center, Massachusetts Institute of Technology, Cambridge MA 02139, USA

The dynamics of electron-plasma waves are described at arbitrary collisionality by considering the full Coulomb collision operator. The description is based on a Hermite-Laguerre decomposition of the velocity dependence of the electron distribution function. The damping rate, frequency, and eigenmode spectrum of electron-plasma waves are found as functions of the collision frequency and wavelength. A comparison is made between the collisionless Landau damping limit, the Lenard-Bernstein and Dougherty collision operators, and the electron-ion collision operator, finding large deviations in the damping rates and eigenmode spectra. A purely damped entropy mode, characteristic of a plasma where pitch-angle scattering effects are dominant with respect to collisionless effects, is shown to emerge numerically, and its dispersion relation is analytically derived. It is shown that such a mode is absent when simplified collision operators are used, and that like-particle collisions strongly influence the damping rate of the entropy mode.

1. Introduction

Electron-plasma waves (EPW), also called Langmuir waves or plasma oscillations, are oscillations of the electron density at the plasma frequency resulting from the break of local charge neutrality (Bohm & Gross 1949; Malmberg & Wharton 1966). The displacement of electrons leads to an electrostatic force that, by pulling electrons back to their equilibrium position, results into oscillations of the electrostatic potential and electron density. In a collisionless system, the amplitude of EPW decreases with time due to Landau damping (Landau 1946). The phenomenon of collisionless Landau damping is well understood, both linearly and non-linearly (Dawson 1961; O’Neil & Rostoker 1965; Zakharov 1972; Morales & O’Neil 1972; Mouhot & Villani 2011). When Coulomb collisions are present, although collisional and Landau damping of EPW are known to act synergistically (Brantov *et al.* 2012), the physical mechanisms which dictate their interplay are considerably less understood. This is despite the fact that plasmas are all characterized by a finite number of particles in a Debye sphere, $N = (4\pi/3)n\lambda_D^3$, with n the electron density and λ_D the Debye length, and therefore collisional effects are always present. Indeed, understanding the behavior of EPW with collisions is important since Coulomb collisions significantly contribute to the behavior of many important laboratory plasmas, such as magnetic

† Email address for correspondence: rogerio.jorge@epfl.ch

‡ Now present at Institute for Research in Electronics and Applied Physics, University of Maryland, College Park MD 20742, USA

(Scott 2007) and inertial fusion (Lindl *et al.* 2004) plasmas, and plasmas for industrial processing (Lieberman & Lichtenberg 2005). Collisions also influence the dynamics of EPW in near-earth space plasmas (Jordanova *et al.* 1996), and can even be the only source of significant damping of EPW in low-temperature laboratory plasmas (Banks *et al.* 2017).

The need for a simplified theoretical framework able to describe Coulomb collisions at arbitrary collisionality is widely recognized, and has been the subject of considerable interest over the past few decades (Callen & Kissick 1997; Ji & Held 2010), with a large effort devoted not only to the study of EPW (Hammett & Perkins 1990; Brantov *et al.* 2012; Banks *et al.* 2016), but also to ion-acoustic waves (Epperlein *et al.* 1992; Tracy *et al.* 1993; Zheng & Yu 2000), and drift-waves (Jorge *et al.* 2018). The difficulty associated with an accurate estimate of the collisional damping in a plasma at arbitrary collisionalities is related to the integro-differential character of the Coulomb collision operator $C(f)$ (Helander & Sigmar 2005). While progress can be made using fluid models that rely on the evaluation of the velocity moments of the kinetic equation (Braginskii 1965), the standard formulation of these models based on collisional closures assumes that typical wave-numbers k of the system are small compared with the inverse mean-free path $1/\lambda_{mfp_a} = \nu_a/v_{tha}$, with ν_a the collision frequency and v_{tha} the thermal velocity of the species a , and that typical frequencies ω are small compared with ν_a . This restricts the application of standard fluid models to highly collisional regimes, therefore excluding Landau damping effects. In order to incorporate kinetic effects in fluid models, closures that mimic the linear response of a collisionless plasma have been derived (Hammett *et al.* 1992, 1993), later extended to include fourth order moments (Hunana *et al.* 2018), and to include collisional effects without pitch-angle scattering (Joseph & Dimits 2016).

A possible approach to the study of the kinetic properties of EPW is based on the development of the distribution function on a convenient basis, and the projection of the kinetic equation on this basis. Indeed, pseudospectral decompositions that expand the electron distribution function in an appropriate orthogonal polynomial basis have allowed a rigorous assessment of the effect of collisional pitch-angle scattering in linear EPW and ion-acoustic waves by including electron-ion collisions while neglecting electron-electron collisions (justified in a high- Z regime) (Epperlein *et al.* 1992; Banks *et al.* 2016). The role of self-collisions in the linear regime was investigated in Banks *et al.* (2017) using a simplified operator with respect to the full Coulomb operator and in Brantov *et al.* (2012) where a simplified form for the high order moments of the like-species Coulomb collision operator was employed in order to derive an analytic dispersion relation.

In this work, the linear properties of EPW are assessed by using the full linearized Coulomb electron-electron and electron-ion collision operators at arbitrary collision frequencies. For this purpose, a pseudospectral decomposition of the electron distribution function based on a Hermite-Laguerre polynomial basis is used. Leveraging the work in Jorge *et al.* (2017, 2018), a moment expansion of the full Coulomb collision operator is performed at all orders by taking into account both like-species and inter-particle collisions without simplifying assumptions. The framework used here allows, for the first time, the evaluation of the frequency and damping rates and, more generally, of the linear spectrum, of EPW eigenmodes, at arbitrary collisionalities. Among the subdominant modes, we focus on the analytical and numerical description of the entropy mode, a purely damped mode that requires the Coulomb collision operator to be properly described (Epperlein 1994; Banks *et al.* 2016). The entropy mode can have a damping rate comparable to other modes in the plasma [such as ion-acoustic waves (Tracy *et al.* 1993)] and similar wave-numbers, and it determines the damping rate of the system on collisional time scales. In fact, as we show, this mode is absent when the kinetic equation is solved using approximate collision

operators or in one-dimensional velocity space descriptions and, in general, deviations between the results based on the Coulomb and simplified collision operators (such as the Lenard-Bernstein, the Dougherty, and the electron-ion operators) are particularly evident. We remark that the discrepancies in the spectrum observed between different collision operators may lead to major differences in the nonlinear evolution of EPW. Indeed, stable modes can be non-linearly excited to a finite amplitude and have a major role in nonlinear energy dissipation and turbulence saturation, affecting the formation of turbulent structures, as well as heat and particle transport (Terry *et al.* 2006; Hatch *et al.* 2011). As a test of our numerical investigations, the results for the Lenard-Bernstein case are compared to the eigenmode spectrum resulting from an analytical solution where the plasma distribution function and the electrostatic potential are decoupled. This also allows us to gain some insight on previous EPW results using the Lenard-Bernstein operator (Bratanov *et al.* 2013; Schekochihin *et al.* 2016). In addition, we compare our pseudospectral decomposition to the one based on a Legendre polynomial expansion for the case of the electron-ion operator.

This paper is organized as follows. Section 2 presents the moment-hierarchy equation used for the EPW description, deriving it from the kinetic Boltzmann equation by using a Hermite-Laguerre expansion of the electron distribution function. Section 3 focuses on the collisionless moment-hierarchy and derives the collisionless dispersion relation. In Section 4, the oscillation frequency and damping rates of EPW are analyzed and compared with simplified collision operators. Section 5 derives a dispersion relation for the entropy mode that shows remarkable agreement with the numerical results. Finally, Section 6 shows the EPW eigenvalue spectrum using different collision operators and discretization methods. The conclusions follow.

2. Moment-Hierarchy Formulation of EPW

We briefly describe the Boltzmann-Poisson system, our starting point for the description of EPW, for an unmagnetized plasma, and derive a moment expansion of the distribution function that allows its numerical solution. The Boltzmann equation for the evolution of the electron distribution function f is given by

$$\frac{\partial f}{\partial t} + \mathbf{v} \cdot \nabla f + \frac{e}{m} \nabla \phi \cdot \frac{\partial f}{\partial \mathbf{v}} = \hat{C}(f). \quad (2.1)$$

In Eq. (2.1), e is the elementary charge, m the electron mass, ϕ the electrostatic potential, and $\hat{C}(f)$ the non-linear Coulomb (also called Landau) collision operator for electrons

$$\hat{C}(f) = \frac{v_{th}^3}{n} \sum_b \nu_b \partial_{\mathbf{v}} \cdot \left[\frac{m}{m_b} (\partial_{\mathbf{v}} H_b) f - \partial_{\mathbf{v}} (\partial_{\mathbf{v}} G_b) \cdot \partial_{\mathbf{v}} f \right], \quad (2.2)$$

where $v_{th} = \sqrt{2T/m}$ is the electron thermal velocity with T the electron temperature, and ν_b the characteristic collision frequency between electrons and species b ($b = e, i$ for electrons and ions, respectively), defined by

$$\nu_e = \frac{8\sqrt{\pi}}{3\sqrt{m_e}} \frac{n\lambda e^4}{T^{3/2}}, \quad (2.3)$$

with λ the Coulomb logarithm and $\nu_i = \sqrt{2}\nu_e$. $H_b = 2 \int f_b(\mathbf{v}')/|\mathbf{v} - \mathbf{v}'| d\mathbf{v}'$ and $G_b = \int f_b(\mathbf{v}')|\mathbf{v} - \mathbf{v}'| d\mathbf{v}'$ are the Rosenbluth potentials (Helander & Sigmar 2005). We relate

the electrostatic potential ϕ to f using Poisson's equation

$$\nabla^2\phi = 4\pi e \left(\int f d\mathbf{v} - n_0 \right), \quad (2.4)$$

where the ions are assumed to provide a fixed homogeneous, neutralizing background, with density n_0 and a Maxwellian-Boltzmann equilibrium with the same temperature as the electrons. An atomic number $Z = 1$ is considered. Equation (2.1) is linearized by expressing f as $f = f_M(1 + \delta f)$ with $\delta f \ll 1$ and f_M an isotropic Maxwell-Boltzmann equilibrium distribution with constant density n_0 and temperature T_0 , yielding

$$f_M \frac{\partial \delta f}{\partial t} + f_M \mathbf{v} \cdot \nabla \delta f + \frac{e}{m} \nabla \delta \phi \cdot \frac{\partial f_M}{\partial \mathbf{v}} = C(f_M \delta f), \quad (2.5)$$

where we used the fact that $\hat{C}(f_M) = 0$, and $C(f_M \delta f)$ is the linearized version of the Coulomb collision operator in Eq. (2.2) whose expression can be found in Helander & Sigmar (2005). The Boltzmann equation, Eq. (2.5), is coupled to the Poisson equation $\nabla^2 \delta \phi = 4\pi e \delta n$ with $\delta n = \int f_M \delta f d\mathbf{v}$ the perturbed electron density. We now rewrite Eq. (2.5) in terms of the Fourier transformed distribution function $\delta f_k = \int \delta f \exp(-i\mathbf{k} \cdot \mathbf{x}) d\mathbf{x}$ as

$$\frac{\partial \delta f_k}{\partial t} + i\mathbf{k} \cdot \mathbf{v} \delta f_k + i\mathbf{k} \cdot \mathbf{v} \frac{4\pi e^2 \delta n_k}{k^2 T_0} = \frac{C(f_M \delta f_k)}{f_M}, \quad (2.6)$$

where we used the Fourier transformed Poisson equation $-k^2 \delta \phi_k = 4\pi e \delta n_k$, with $\delta n_k = \int \delta n \exp(-i\mathbf{k} \cdot \mathbf{x}) d\mathbf{x}$ and $\delta \phi_k = \int \delta \phi \exp(-i\mathbf{k} \cdot \mathbf{x}) d\mathbf{x}$.

Similarly to previous studies on the collisional damping of EPW (Brantov *et al.* 2012; Banks *et al.* 2016), a three-dimensional cylindrical (v_\perp, φ, v_z) velocity coordinate system is used, therefore decomposing the velocity vector \mathbf{v} as

$$\mathbf{v} = v_z \mathbf{e}_z + v_\perp (\cos \varphi \mathbf{e}_x + \sin \varphi \mathbf{e}_y), \quad (2.7)$$

where $(\mathbf{e}_x, \mathbf{e}_y, \mathbf{e}_z)$ are Cartesian unit vectors with z the direction of the wave-vector $\mathbf{k} = k\mathbf{e}_z$. In this work, we consider the azimuthally isotropic, i.e. φ independent, subset of solutions $\delta f_k = \delta f_k(v_\perp, v_z)$ of the Boltzmann equation, Eq. (2.6), which further allows us to reduce our study to the one of a two-dimensional model. This can be done by applying the averaging operator $\langle \dots \rangle$ defined by

$$\langle g \rangle (v_\perp, v_z) = \frac{1}{2\pi} \int_0^{2\pi} g(v_\perp, \varphi, v_z) d\varphi, \quad (2.8)$$

to the Boltzmann equation, Eq. (2.5), yielding

$$\frac{\partial \langle \delta f_k \rangle}{\partial t} + ikv_z \langle \delta f_k \rangle + ikv_z \frac{4\pi e^2 \delta n_k}{k^2 T_0} = \frac{\langle C(f_M \delta f_k) \rangle}{f_M}. \quad (2.9)$$

As the linearized Coulomb collision operator satisfies $\langle C(f_M \delta f_k) \rangle = C(f_M \langle \delta f_k \rangle)$, Eq. (2.9) can be used to obtain the subset of azimuthally symmetric solutions in velocity space $\langle \delta f_k \rangle$, which are decoupled from the azimuthally asymmetric solutions $\delta \tilde{f}_k = \delta f_k - \langle \delta f_k \rangle$. Finally, we rewrite Eq. (2.9) by normalizing time to kv_{th0} with $v_{th0} = \sqrt{2T_0/m}$ the electron thermal velocity, δn_k to n_0 , and v_z to v_{th} , yielding

$$i \frac{\partial \langle \delta f_k \rangle}{\partial t} - v_z \langle \delta f_k \rangle - \frac{v_z \delta n_k}{\alpha_D} = i \frac{\langle C(f_M \delta f_k) \rangle}{f_M}, \quad (2.10)$$

where we defined $\alpha_D = k^2 \lambda_D^2$ with $\lambda_D = \sqrt{T_0/(4\pi e^2 n_0)}$ the Debye length, and where the

collision frequency coefficient present in $C(f_M \delta f_k)$ is now in units of kv_{th} . Furthermore, we define ν as the electron-ion collision frequency normalized to kv_{th} , namely

$$\nu = \frac{\nu_i}{kv_{th}}. \quad (2.11)$$

We note that the number of particles in a Debye-sphere N can be cast in terms of ν and α_D as

$$N = \frac{1}{9} \sqrt{\frac{2}{\pi}} \frac{\lambda}{\nu \sqrt{\alpha_D}}, \quad (2.12)$$

where λ is the Coulomb logarithm.

Following Jorge *et al.* (2017, 2018), we solve the linearized kinetic equation, Eq. (2.10), at arbitrary collisionalities by expanding the perturbed distribution function $\langle \delta f_k \rangle$ into an orthogonal Hermite-Laguerre polynomial basis of the form

$$\langle \delta f_k \rangle = \sum_{p,j=0}^{\infty} \frac{N^{pj}}{\sqrt{2^p p!}} H_p(v_z) L_j(v_{\perp}^2), \quad (2.13)$$

where H_p are *physicists'* Hermite polynomials of order p , defined by the Rodrigues' formula

$$H_p(x) = (-1)^p e^{x^2} \frac{d^p}{dx^p} e^{-x^2}, \quad (2.14)$$

and normalized via the orthogonality condition based on the scalar product with weight factor e^{-x^2}

$$\int_{-\infty}^{\infty} dx H_p(x) H_{p'}(x) e^{-x^2} = 2^p p! \sqrt{\pi} \delta_{pp'}, \quad (2.15)$$

and L_j the Laguerre polynomials of order j , defined by the corresponding Rodrigues' formula

$$L_j(x) = \frac{e^x}{j!} \frac{d^j}{dx^j} (e^{-x} x^j), \quad (2.16)$$

and orthonormal with respect to the weight e^{-x}

$$\int_0^{\infty} dx L_j(x) L_{j'}(x) e^{-x} = \delta_{jj'}. \quad (2.17)$$

Due to the orthogonality of the Hermite-Laguerre basis, the coefficients $N^{pj} = N^{pj}(k, t)$ of the expansion in Eq. (2.13) can be computed via the expression

$$N^{pj} = \int \frac{H_p(v_z) L_j(v_{\perp}^2) \langle \delta f_k \rangle}{\sqrt{2^p p!}} \frac{e^{-v_z^2 - v_{\perp}^2}}{\sqrt{\pi}} dv_z dv_{\perp}^2. \quad (2.18)$$

With respect to a grid treatment using collocation points based on orthogonal polynomials (Belli & Candy 2008; Landreman & Ernst 2013), we note that the Hermite-Laguerre decomposition used in this work allows us to find the Rosenbluth potentials analytically as linear combinations of the N^{pj} moments of the distribution function, to find linear and nonlinear closures at an arbitrary number of moments and mean-free path, and to make much more evident the role of the parallel and perpendicular phase-mixing processes.

By projecting the Boltzmann equation, Eq. (2.10), onto a Hermite-Laguerre basis, a system of differential equations (henceforth called moment-hierarchy) for the coefficients N^{pj} is obtained

$$i \frac{\partial}{\partial t} N^{pj} = \sqrt{\frac{p+1}{2}} N^{p+1j} + \sqrt{\frac{p}{2}} N^{p-1j} + \frac{N^{00}}{\alpha_D} \frac{\delta_{p,1} \delta_{j,0}}{\sqrt{2}} + i C^{pj}, \quad (2.19)$$

with C^{pj} the projection of the linearized collision operator onto a Hermite-Laguerre basis

$$C^{pj} = \int \frac{H_p(v_z) L_j(v_\perp^2) \langle C(f_M \delta f_k) \rangle}{\sqrt{2^p p!}} dv_z dv_\perp^2. \quad (2.20)$$

The Coulomb collisional moments C^{pj} are derived leveraging the result in Ji & Held (2006), where the collision operator is projected onto a tensorial basis of the form $\mathbf{p}^{ls} = \mathbf{P}^l(\mathbf{c}) L_s^{l+1/2}(c^2)$, with the irreducible tensorial Hermite polynomials defined by the recurrence $\mathbf{P}^{l+1}(\mathbf{c}) = \mathbf{c} \mathbf{P}^l(\mathbf{c}) - c^2 \partial_{\mathbf{c}} \mathbf{P}^l(\mathbf{c}) / (2l + 1)$, being $\mathbf{P}^0(\mathbf{c}) = 1$ with $\mathbf{c} = \mathbf{v}/v_{th}$, and the associated Laguerre polynomials $L_s^{l+1/2}(x) = \sum_{m=0}^s L_{sm}^l x^m$ with $L_{sm}^l = [(-1)^m (l + s + 1/2)!] / [(s - m)! (l + m + 1/2)! m!]$. Indeed, expanding the distribution function as $\delta f_a = \sum_{l,s} \mathbf{M}_a^{ls} \cdot \mathbf{p}^{ls} / \sigma_s^l$, and with $\sigma_s^l = l!(l + s + 1/2)! / (2^l (l + 1/2)! s!)$, Ji and Held showed that the linearized collision operator can be written as

$$C(f_M \delta f) = f_M \sum_b \sum_{l,s=0}^{\infty} \frac{\mathbf{P}^l(\hat{v})}{\sigma_s^l} \cdot \left(\mathbf{M}_e^{ls} \nu_{eb}^{ls,0} + \mathbf{M}_b^{ls} \nu_{eb}^{0,ls} \right). \quad (2.21)$$

where $\nu_{eb}^{ls,0}(v)$ and $\nu_{eb}^{0,ls}(v)$ are linear combinations of the error function and its derivatives [for their expression, see Ji & Held (2006)], and represent the test-particle and field-particle (back-reaction) parts of the linearized collision operator, respectively. We remark that a similar expansion in Legendre-Associated Laguerre polynomials was used in Brantov *et al.* (2012) in order to derive a simplified dispersion relation applicable to the study of EPW, ion-acoustic waves, and entropy modes.

In order to evaluate C^{pj} , we Fourier transform in space and average the operator $C(f_M \delta f)$ in Eq. (2.21) according to Eq. (2.8), using the averaging identity $\langle \mathbf{P}^l(\mathbf{c}) \rangle = c^l P_l(v_z/v) \mathbf{P}^l(\hat{e}_z)$, with $P_l(x) = \partial_x^l (x^2 - 1)^l / (2^l l!)$ the Legendre polynomials. This yields

$$\langle C(f_M \delta f_k) \rangle = \sum_b \sum_{l,s=0}^{\infty} (C_{eb}^{ls,0} + C_{eb}^{0,ls}), \quad (2.22)$$

where $C_{eb}^{ls,0}$ is the averaged test-particle operator

$$C_{eb}^{ls,0} = f_M \nu_{eb}^{ls,0}(v) P_l\left(\frac{v_z}{v}\right) M_e^{ls} \frac{2^l (l!)^2}{(2l)!}, \quad (2.23)$$

and $C_{eb}^{0,ls}$ the field-particle (back-reaction) operator

$$C_{eb}^{0,ls} = f_M \nu_{eb}^{0,ls}(v) P_l\left(\frac{v_z}{v}\right) M_b^{ls} \frac{2^l (l!)^2}{(2l)!}, \quad (2.24)$$

with the fluid moments defined as

$$M_b^{ls} = \sum_{p=0}^{l+2s} \sum_{j=0}^{s+l/2} T_{ls}^{pj} N_b^{pj} \sqrt{\frac{2^p p!}{\sigma_s^l}}. \quad (2.25)$$

The basis transformation coefficients T_{ls}^{pj} in Eq. (2.25) are defined by

$$v^l P_l\left(\frac{v_z}{v}\right) L_s^{l+1/2}(v^2) = \sum_{p=0}^{l+2s} \sum_{j=0}^{s+l/2} T_{ls}^{pj} H_p(v_z) L_j(v_\perp^2), \quad (2.26)$$

and their closed form expression can be found in Jorge *et al.* (2017). While an expansion in tensorial Hermite polynomials $\mathbf{P}^l(\mathbf{c})$ allows us to conveniently express the linearized collision operator in terms of M_b^{ls} moments, the basis transformation of Eq. (2.26) is

needed to cast the velocity dependence of $\langle C(f_M \delta f_k) \rangle$ in a Hermite-Laguerre polynomial basis, and to calculate its velocity moments.

We now use the expression of $\langle C(f_M \delta f_k) \rangle$ contained in Eq. (2.22) and inject it in Eq. (2.18). By defining the fluid moments A_{eb}^{lts} as

$$A_{eb}^{lts} = \int v^l L_t^{l+1/2}(v^2) f_M \nu_b^{ls,0}(v) dv, \quad (2.27)$$

and B_{eb}^{lts} as

$$B_{eb}^{lts} = \int v^l L_t^{l+1/2}(v^2) f_M \nu_b^{0,ls}(v) dv, \quad (2.28)$$

the resulting collision operator moments C^{pj} can be written as

$$C^{pj} = \sum_b \sum_{s=0}^{\infty} \sum_{l=0}^{p+2j} \sum_{t=0}^{j+[p/2]} \frac{(T^{-1})_{pj}^{lt} 2^l (l!)^2}{(2l)! \sigma_s^l \sqrt{2^p p!}} \frac{\nu_b}{(2l+1)} (M_e^{ls} A_{eb}^{lts} + M_b^{ls} B_{eb}^{lts}), \quad (2.29)$$

where we introduce the inverse transformation coefficients

$$(T^{-1})_{pj}^{lt} = T_{lt}^{pj} \frac{\sqrt{\pi} 2^p p! (l+1/2)!}{(t+l+1/2)!}. \quad (2.30)$$

The analytical expressions for A_{eb}^{lts} and B_{eb}^{lts} suitable for numerical implementation are given in Ji & Held (2006). The moments of the collision operator, C^{pj} , correspond to the ones derived in Jorge *et al.* (2018) for the study of drift-waves, and can also be obtained by linearizing the electron collisional moments presented in Jorge *et al.* (2017).

Besides the Coulomb collision operator, the Hermite-Laguerre expansion described above can be advantageously applied to describe other collision operators. We consider here the Lenard-Bernstein (Lenard & Bernstein 1958), the Dougherty (Dougherty 1964), and the electron-ion collision operators that are used for comparison with the full Coulomb one. The Lenard-Bernstein and Dougherty operators are implemented in a number of advanced kinetic codes (Nakata *et al.* 2016; Grandgirard *et al.* 2016; Loureiro *et al.* 2016; Pan *et al.* 2018), and are frequently used to introduce collisional effects in weakly collisional plasmas (Zocco & Schekochihin 2011; Zocco *et al.* 2015; Shi *et al.* 2017; Mandell *et al.* 2018). Therefore, a comparison between the Coulomb and the Lenard-Bernstein and Dougherty operators, even in simplified systems such as the case of EPW, is important to determine the accuracy and validity of these operators. The Lenard-Bernstein collision operator $C_{LB}(f)$, first derived in 1891 by L. Rayleigh (Wax 1954) is of the Fokker-Planck type. It conserves particle number and satisfies the H-theorem, and it can be written as (Lenard & Bernstein 1958)

$$C_{LB}(f) = \nu \frac{\partial}{\partial \mathbf{v}} \cdot \left(\mathbf{v} f + \frac{v_{th}^2}{2} \frac{\partial f}{\partial \mathbf{v}} \right). \quad (2.31)$$

This operator can be derived from the Fokker-Planck equation, Eq. (2.2), by assuming $(m/m_b) \partial_{\mathbf{v}} H_b = \mathbf{v}$ and $\partial_{\mathbf{v}} \partial_{\mathbf{v}} G_b = -\mathbf{I} v_{th}^2 / 2$ with \mathbf{I} the identity matrix. By projecting the Lenard-Bernstein operator onto a Hermite-Laguerre basis according to Eq. (2.20), one obtains

$$C_{LB}^{pj} = -\nu(p+2j)N^{pj}. \quad (2.32)$$

Equation (2.32) can then be used in the moment-hierarchy equation Eq. (2.19), yielding

$$i \frac{\partial}{\partial t} N^{pj} = \sqrt{\frac{p+1}{2}} N^{p+1j} + \sqrt{\frac{p}{2}} N^{p-1j} + \frac{N^{00}}{\alpha_D} \frac{\delta_{p,1} \delta_{j,0}}{\sqrt{2}} - i\nu(p+2j)N^{pj}. \quad (2.33)$$

The linearized Dougherty collision operator $C_D(f)$, on the other hand, adds the necessary field-particle collisional terms to the Lenard-Bernstein operator in order to provide momentum and energy conservation properties. Namely, it sets $(m/m_b)\partial_{\mathbf{v}}H_b = \mathbf{v} - \mathbf{u}$, with $\mathbf{u} = \int \mathbf{v} f dv_z dv_{\perp}^2 d\varphi/n_0$, and $\partial_{\mathbf{v}}\partial_{\mathbf{v}}G_b = -\mathbf{IT}/m_a$ with $T = \int m(\mathbf{v} - \mathbf{u})^2 f dv_z dv_{\perp}^2 d\varphi/(3n_0) = (\sqrt{2}N^{20} - 2N^{01})/3$. The Hermite-Laguerre moments of the linearized Dougherty collision operator C_D^{pj} are given by

$$C_D^{pj} = -\nu \left[(p+2j)N^{pj} - N^{10}\delta_{p1}\delta_{j0} + T(\sqrt{2}\delta_{p0}\delta_{j1} - 2\delta_{p2}\delta_{j0}) \right], \quad (2.34)$$

yielding the moment-hierarchy equation

$$i\frac{\partial}{\partial t}N^{pj} = \sqrt{\frac{p+1}{2}}N^{p+1j} + \sqrt{\frac{p}{2}}N^{p-1j} + \frac{N^{00}}{\alpha_D} \frac{\delta_{p,1}\delta_{j,0}}{\sqrt{2}} - i\nu \left[(p+2j)N^{pj} - N^{10}\delta_{p1}\delta_{j0} + T(\sqrt{2}\delta_{p0}\delta_{j1} - 2\delta_{p2}\delta_{j0}) \right]. \quad (2.35)$$

We note that the moment-hierarchies with the Lenard-Bernstein or the Dougherty collision operator, Eq. (2.33) and Eq. (2.35), respectively, do not couple different Laguerre moments and, therefore, one can focus on obtaining the coefficients N^{p0} for solving the moment-hierarchy.

The Hermite-Laguerre expansion procedure can also be applied to the electron-ion operator $C_{ei}(f)$ that is often used for EPW studies (Epperlein *et al.* 1992; Banks *et al.* 2016), that is

$$C_{ei}(f) = \frac{\nu}{2v^3} \frac{\partial}{\partial \xi} \left[(1 - \xi^2) \frac{\partial f}{\partial \xi} \right], \quad (2.36)$$

with $\xi = v_z/v$. This operator describes the pitch-angle scattering of electrons due to collisions with ions. By projecting Eq. (2.36) into a Hermite-Laguerre basis, we obtain (Jorge *et al.* 2017)

$$C_{ei}^{pj} = -\frac{\nu}{8\pi^{3/2}} \sum_{l=0}^{p+2j} \sum_{f=0}^{j+\lfloor p/2 \rfloor} \frac{(T^{-1})_{pj}^{lf}}{\sqrt{2^p p!}} \sum_{s=0}^{\infty} A_{ei}^{lf,s} M_e^{ls}, \quad (2.37)$$

where the $A_{ei}^{lf,s}$ coefficients are given by

$$A_{ei}^{lf,s} = \frac{l(l+1)}{l+1/2} \frac{2^l (l!)^2}{(2l)!} \sum_{m=0}^f \sum_{n=0}^s \frac{L_{fm}^l L_{sn}^l}{\sqrt{\sigma_s^l}} (l+m+n-1)!. \quad (2.38)$$

As an aside, we note that previous studies on EPW have shown that the solutions of the linearized Boltzmann equation are, in fact, sensitive to the discretization method used. For example, it was shown that finite-difference methods, when applied to the problem of EPW, produce a number of numerical, non-physical modes with a rather small damping rate that do not lie in the vicinity of the collisionless solutions, even for weak collisionalities and a very high resolution (Bratanov *et al.* 2013). On the other hand, a discretization scheme based on a Hermite-Laguerre polynomial decomposition yields a large number of roots that lie in the vicinity of the collisionless solution. Since previous EPW studies using the electron-ion collision operator have been performed using a discretization of the distribution function into a set of Legendre polynomials, i.e., (Epperlein *et al.* 1992; Brantov *et al.* 2012; Banks *et al.* 2016)

$$\langle \delta f_k \rangle = \sum_{l=0}^{\infty} a_l(v) P_l(\xi), \quad (2.39)$$

as a test of our approach, we compare in Section 6 our results with the Legendre decomposition in Eq. (2.39). By projecting the Boltzmann equation, Eq. (2.10), with an electron-ion collision operator into a Legendre basis, Eq. (2.39), the following moment-hierarchy equation is obtained

$$\frac{i}{v} \frac{da_l(v)}{dt} = \frac{l}{2l-1} a_{l-1}(v) + \frac{l+1}{2l+3} a_{l+1}(v) + \frac{\delta_{l,1}}{\alpha_D} \int f_M v^2 a_0(v) dv - \frac{i\nu}{v^4} l(l+1) a_l. \quad (2.40)$$

A relation between the Hermite-Laguerre N^{pj} and Legendre moments a_l can be found by comparing Eqs. (2.13) and (2.39), yielding

$$a_l(v) = \sum_{p=0}^{\infty} \sum_{j=0}^{\infty} \sum_{s=0}^{p+2j} \sum_{t=0}^{j+[p/2]} (T^{-1})_{pj}^{st} \frac{N^{pj}}{\sqrt{2^p p!}} v^s L_t^{s+1/2}(v^2) \delta_{ls}, \quad (2.41)$$

and

$$N^{pj} = \sum_{s=0}^{p+2j} \sum_{t=0}^{j+[p/2]} \frac{(T^{-1})_{pj}^{st}}{\sqrt{2^p p!} (2l+1)} \int a_s(v) v^{s+2} L_t^{s+1/2}(v^2) dv. \quad (2.42)$$

3. Collisionless Dispersion Relation

As a first step in the analysis of EPW, and for comparison with the results in the presence of collisions, we derive the EPW dispersion relation in the collisionless limit. We first Fourier transform in time the collisionless limit of the moment-hierarchy equation, Eq. (2.19), by imposing $\delta f_k \sim e^{(\gamma+i\omega)t}$, obtaining

$$i(\gamma+i\omega)N^{pj} = \sqrt{\frac{p+1}{2}} N^{p+1j} + \sqrt{\frac{p}{2}} N^{p-1j} + \frac{N^{00}}{\alpha_D} \frac{\delta_{p,1} \delta_{j,0}}{\sqrt{2}}. \quad (3.1)$$

A closed form solution of the collisionless moment-hierarchy in Eq. (3.1) can be obtained by dividing the Boltzmann equation, Eq. (2.10), by the resonant $i\gamma - v_z$ factor, multiplying it by the Hermite-Laguerre polynomial basis functions and, finally, integrating it over velocity space. This yields

$$N^{pj} = -\frac{N^{00}}{\alpha_D} \left[-i(\gamma+i\omega) \frac{(-1)^p}{\sqrt{2^p p!}} Z^{(p)}(\omega-i\gamma) + \delta_{p,0} \right] \delta_{j,0}, \quad (3.2)$$

where $Z^{(p)}$ is the p th derivative of the plasma dispersion function $Z^{(0)}$, defined by

$$Z^{(p)}(u) = \frac{(-1)^p}{\sqrt{\pi}} \int_{-\infty}^{\infty} \frac{H_p(x) e^{-x^2}}{x-u} dx. \quad (3.3)$$

By setting $(p, j) = (0, 0)$ in Eq. (3.2), the collisionless dispersion relation is found

$$D = 1 + \alpha_D - i(\gamma+i\omega)Z(\omega-i\gamma) = 0. \quad (3.4)$$

Alternatively, Eq. (3.4) can be derived from the collisionless limit of the Boltzmann equation, Eq. (2.10), upon division by the factor $i\gamma - \omega - v_z$ and integration with respect to v_z . The numerical solution of Eq. (3.4) is obtained by discretizing γ and ω into a two-dimensional $[\omega, \gamma]$ grid, evaluating D on the grid, and storing the values where $[Re(D), Im(D)]$ vanishes. To evaluate Z , we make use of the identity $Z(x) = i\sqrt{\pi} e^{-x^2} \operatorname{erfc}(-ix)$ with $\operatorname{erfc}(x) = 1 - \operatorname{erf}(x)$ and $\operatorname{erf}(x)$ the error function, and use the algorithm developed in Gautschi (1970) to numerically compute $\operatorname{erf}(x)$ for complex arguments.

The α_D dependence of the least damped solution of Eq. (3.4) is shown in Fig. 1, where

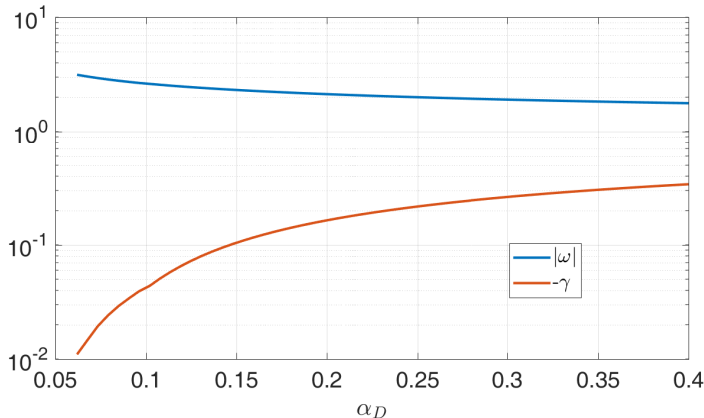


FIGURE 1. Collisionless frequency (blue line) and damping rate (red line) of the least damped solution of the collisionless dispersion relation, Eq. (3.4), as a function of α_D , for $0.05 < \alpha_D < 0.4$.

both its damping rate γ and frequency ω are seen to be monotonic functions of α_D , which is in agreement with previous EPW studies (Banks *et al.* 2017). In the following, without loss of generality and similarly to previous studies of collisional damping of EPW (Banks *et al.* 2016, 2017), we select the value of $\alpha_D = 0.09$ when fixed α_D studies are performed, which corresponds to $k\lambda_D = \sqrt{\alpha_D} = 0.3$. While this value of α_D is typical for EPW driven by stimulated Raman scattering (Brunner & Valeo 2004; Winjum *et al.* 2013), we add that the particular choice of α_D has no quantitative impact on the conclusions we draw.

4. Temporal Evolution of EPW

In this section, the moment-hierarchy equation, Eq. (2.19), is solved numerically as a time-evolution problem using an implicit variable-step variable-order solver that employs backward differentiation formulas (Shampine 2002) with a maximum time-step of $10^{-6}kv_{th}$. For the numerical solution, the moment-hierarchy is truncated at a maximum Hermite-Laguerre index (P, J) by setting

$$N^{pj} = 0, \text{ for } (p, j) > (P, J). \quad (4.1)$$

We consider as initial condition $N^{pj}(t=0) = \delta_{p0}\delta_{j0}$, such that the perturbed density and electrostatic potential are initially excited, while higher moments of the distribution function are set to zero. The initial perturbation of the velocity distribution function is then taken to be a Maxwellian in velocity space. The temporal evolution of N^{00} (and therefore of ϕ) is shown in Fig. 2 for different collisionalities and α_D values. In this section, we focus on the oscillating initial phase of Fig. 2, where the EPW dominate the dynamics. We fit the amplitude of N^{00} to an exponentially damped sinusoidal wave with real frequency ω and damping rate γ , taking into account a minimum of three oscillation periods. The later phase, where a purely damped behavior is observed at higher collisionalities due to the presence of an entropy mode, is investigated in Section 5.

A convergence study with the truncation indices (P, J) is shown in Fig. 3. Convergence is observed for $(P, J) = (18, 2)$ in the range of collisionalities and α_D investigated (a variation of less than 3% is observed between damping rates evaluated with a truncation at $(P, J) = (18, 2)$ and a truncation at higher values of P and J). The values of oscillation frequency $\omega(\alpha_D, \nu)$ and damping rate $\gamma(\alpha_D, \nu)$ obtained as a fit of the initial damping

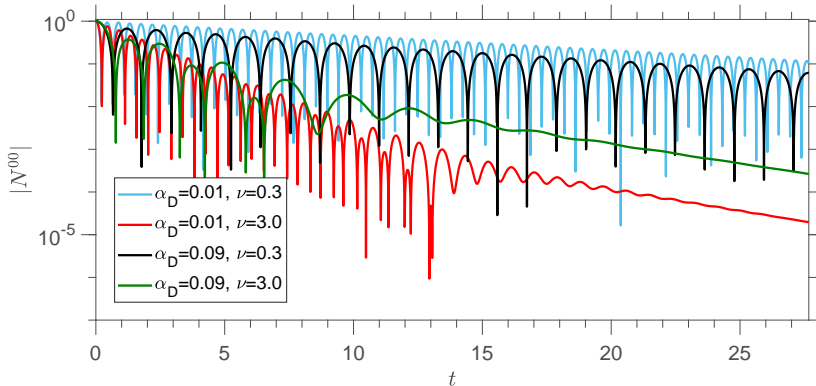


FIGURE 2. Time evolution of the absolute value of N^{00} using a truncation with $(P, J) = (18, 2)$, evaluated using the full linearized Coulomb collision operator. Different values of ν and α_D are shown.

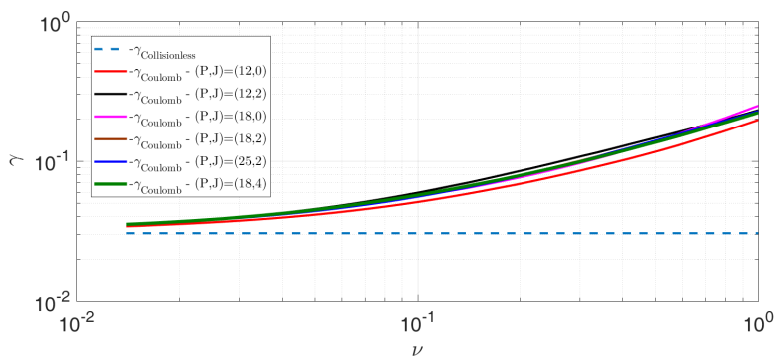


FIGURE 3. Comparison of the normalized damping rate γ for $\alpha_D = 0.09$ as a function of the normalized collision frequency considering a truncation at different values of (P, J) (solid lines) and using the full linearized Coulomb collision operator. The collisionless least damped Landau solution is shown for comparison (dashed blue line). All frequencies are normalized to kv_{th} .

phase are shown in Fig. 4 for $0.075 < \alpha_D < 0.2$ and $0.015 < \nu < 0.7$ using the Coulomb collision operator, where a truncation at $(P, J) = (18, 2)$ is used. Such values of (P, J) are in line with the estimate found in Jorge *et al.* (2018) which, by underestimating the effect of the collisional term C^{pj} in the moment-hierarchy equation leads to $P \sim 4/\sqrt{2}\nu$ and $J \sim 2$. For $\nu \sim 0.1$, this yields $(P, J) \sim (30, 2)$. The largest deviation of the damping rate from the collisionless case is seen to occur for large values of collisionality and small α_D . This is expected, as for large ν and small α_D the collisional fluid limit is retrieved. The dependence on α_D may be attributed to the decreasing magnitude of the Landau damping rate for decreasing α_D (see Fig. 1). This makes the ratio between the collisional and the collisionless damping rates increasingly larger. Finally, we remark that the presence of several competing eigenmodes in the initial transients of the temporal evolution of N^{00} contribute to the presence of a transition at $\alpha_D \sim 0.1$ visible in Fig. 4.

Following a long standing tradition established by Jackson (Jackson 1960), and used in consequent EPW studies (Opher *et al.* 2002), we also display the frequency and the damping rate of EPW normalized to the plasma frequency $\omega_{pe} = v_{th}/\lambda_D$ in Fig. 5 as a function of $k\lambda_D$ for fixed ν_{ei}/ω_{pe} . We show the results for the collisionless $\nu_{ei}/\omega_{pe} = 0$ and the collisional $\nu_{ei}/\omega_{pe} = 0.1$ case. Consistently with Fig. 4, it is observed that ω/ω_{pe}

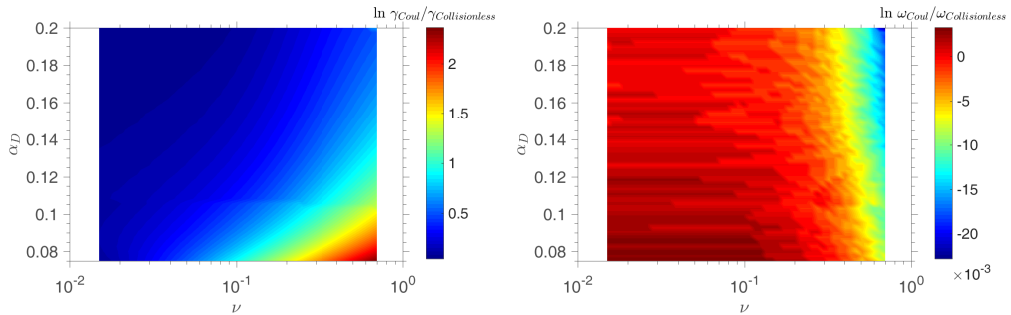


FIGURE 4. Damping rate γ (left) and oscillation frequency ω (right) of the electron-plasma wave obtained from the moment-hierarchy equation, Eq. (2.19), as a function of α_D and ν for $(P, J) = (18, 2)$. The full linearized Coulomb collision operator is considered.

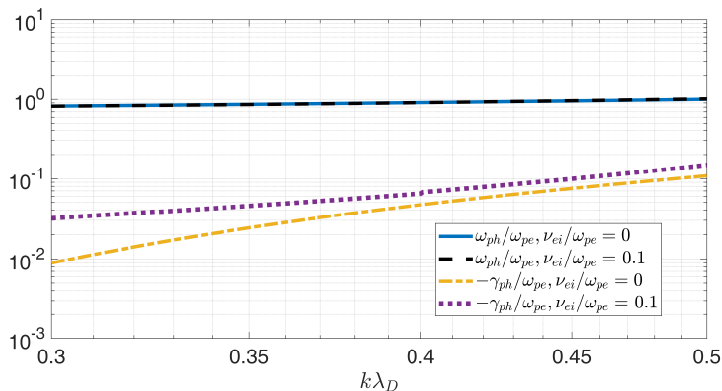


FIGURE 5. Oscillation frequency $\omega_{ph} = k\omega v_{th}$ and damping rate $\gamma_{ph} = \gamma k v_{th}$ of EPW in physical units, normalized to the plasma frequency ω_{pe} for the collisionless $\nu_{ei}/\omega_{pe} = 0$ and collisional $\nu_{ei}/\omega_{pe} = 0.1$ case.

has a negligible relative variation with the collision frequency when compared with the relative variation of the damping rate. Furthermore, as observed in Opher *et al.* (2002), the damping rate of EPW with finite collision frequency is seen to approach the collisionless result for high values of $k\lambda_D$. A further comparison of the collisional component of the damping rate γ_{coll} , obtained with different collision models, is shown in Fig. 6, where $\gamma_{coll} = \gamma - \gamma_{collisionless}$ with γ the total damping rate and $\gamma_{collisionless}$ the collisionless Landau damping. Results considering Lenard-Bernstein, Dougherty, electron-ion, and the full Coulomb collision operators are shown. We note that when the Lenard-Bernstein and the Dougherty operator are considered, only self-collisions are taken into account, and with the electron-ion operator only unlike-particle collisions are included. In general, the Coulomb operator yields a damping rate smaller than the Lenard-Bernstein and larger than the Dougherty one, with deviations of up to 50% between different operators. The use of an electron-ion collision operator is preferable since it yields damping rates and frequencies similar, just slightly lower, than the Coulomb operator. The collisional damping rate, $\gamma_{fluid} = -0.532\nu/2$, obtained from a fluid description using the Braginskii equations (Banks *et al.* 2017), is also shown for comparison. We remark that the results in Fig. 6 for the collisional component of the damping rate of the fluid, purely e-i collisions, and the full Coulomb operator are in close agreement with the findings of Banks *et al.* (2017).

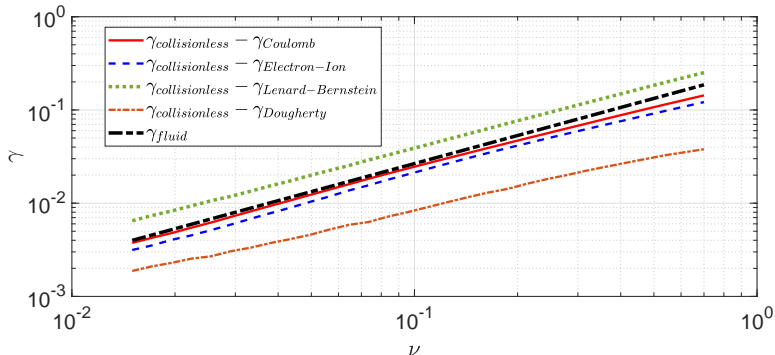


FIGURE 6. Difference between the collisionless damping rate γ with the one resulting from the moment-hierarchy equation, Eq. (2.19), with the full Coulomb, Lenard-Bernstein, Dougherty, and electron-ion collision operators at $\alpha_D = 0.09$ and $(P, J) = (18, 2)$. The collisional damping rate $\gamma_{fluid} = -0.266\nu$ obtained from a fluid description is also shown for comparison.

For $\nu \ll 1$, it is seen that the damping rates of all solutions approach the collisionless limit regardless of the collision operator used. When ν is increased, Fig. 6 shows that the differences between the collision operators still persist. This allows us to draw arguments for the difference between the different collision operators by using a low number of moments. The lowest order particle conservation $C^{00} = 0$ and collisional friction $C^{10} = -\nu N^{10}$ moments C^{pj} are the same between the Coulomb, Lenard-Bernstein, and electron-ion collision operators, while the Dougherty operator has $C_D^{10} = 0$. This effectively reduces the damping rate evaluated with the Dougherty operator with respect to the Coulomb case, as seen in Fig. 6.

On the other hand, only the Coulomb, the Dougherty, and the electron-ion collision operators are energy conserving, i.e., satisfying $(1/2) \int m(v_z^2 + v_\perp^2) C(f) d\mathbf{v} = 0$ or, equivalently, $C^{20} = \sqrt{2} C^{01}$, while the Lenard-Bernstein operator does not conserve energy. In fact, the energy moments are given by $C_{LB}^{01} = -\nu 2N^{01}$ and $C_{LB}^{20} = -\nu 2N^{20}$, yielding $C_{LB}^{01} = C_{LB}^{20}$. However, despite the additional conservation properties, the agreement of the Dougherty operator is rather poor, as seen in Fig. 6. We conclude therefore that the presence of additional momentum and energy conserving terms in the Dougherty operator with respect to the Lenard-Bernstein operator does not yield a damping rate closer to the Coulomb one. This was also pointed out in Jorge *et al.* (2018), where a similar framework was used to derive the growth rate of the drift-wave instability.

5. Entropy Mode

We focus on the latter stage of the time evolution of N^{00} shown in Figs. 2 and 7, where a purely damped behavior is found at high collisionalities. In order to enhance the role of the zero-frequency mode, we consider the collision frequency $\nu = 5$, while decreasing the role of Landau damping by setting $\alpha_D = 0.01$ (the purely damped mode is not affected by the value of α_D , if $\alpha_D \ll 1$). Indeed, the transition to a purely damped behaviour is seen to occur at times that decrease with the collision frequency [see Fig. 7 (black)]. The resulting time traces of $|N^{00}|$ using a full-Coulomb collision operator are shown in Fig. 7 (left) for $(P, J) = (18, 0)$, $(P, J) = (18, 2)$, and $(P, J) = (18, 4)$, while time traces using the full-Coulomb, electron-ion, Lenard-Bernstein and the Dougherty collision operators with $(P, J) = (18, 2)$ are shown in Fig. 7 (right). We observe that for the Coulomb and electron-ion case, there is a transition to a purely damped mode at $t \simeq 7$ only when perpendicular velocity dynamics is introduced, $J \geq 2$. At the same time, while for the

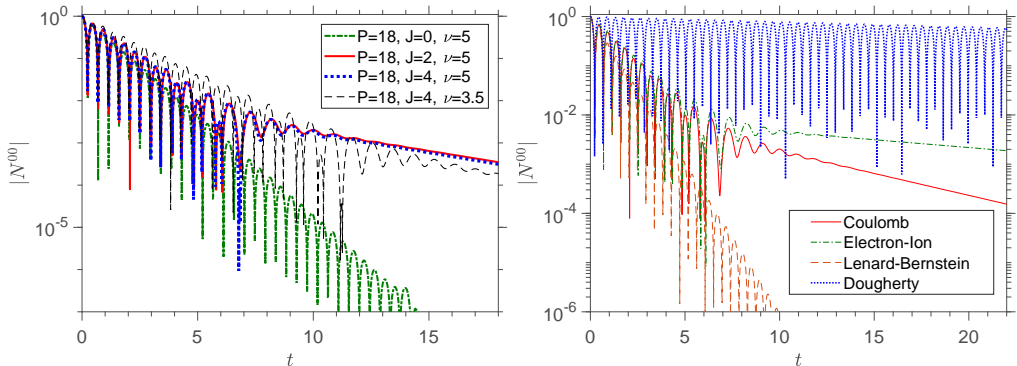


FIGURE 7. Time evolution of the absolute value of N^{00} with $\nu = 5$ and $\alpha_D = 0.01$. Left: convergence study with a full-Coulomb operator and $(P, J) = (18, 0)$ (green), $(P, J) = (18, 2)$ (red), and $(P, J) = (18, 4)$ (blue). The time evolution of N^{00} with $\nu = 3.5$ and $(P, J) = (18, 4)$ is also shown for comparison (black). Right: truncation at $(P, J) = (18, 2)$ using the full-Coulomb collision operator (red), electron-ion collisions only (green), the Lenard-Bernstein (orange) and the Dougherty (blue) collision operators.

Coulomb operator, the purely damped mode that sets the late time evolution of the system in Fig. 7 has a damping rate $\gamma \simeq -0.202$, the electron-ion collision operator yields a damping rate one order of magnitude smaller, $\gamma \simeq -0.024$. This purely damped decay is not present when the Lenard-Bernstein or the Dougherty operators are considered. We therefore conclude that in order to obtain the correct long-term behaviour of the Boltzmann equation, Coulomb self-collisions must be included in the description.

The long term behaviour observed in Fig. 7 is due to the presence of the entropy mode (Banks *et al.* 2016). An analytical framework to model the entropy mode can be derived by noting that this is a purely damped mode with a damping rate much smaller than both the plasma and the collision frequencies. Previous studies on the collisional damping of EPW show that such a mode results from the effect of pitch-angle scattering at high-collisionality (Banks *et al.* 2016). Considering that in the high-collisionality limit only the lowest order terms in the expansion of $\langle \delta f_k \rangle$ in Eq. (2.13) play a role and that, according to Fig. 7, a finite perpendicular velocity-space resolution is an essential element for the entropy mode, we consider in the moment-hierarchy equation, Eq. (2.19), the six lowest order Hermite-Laguerre expansion coefficients, namely $N^{00}, N^{10}, N^{20}, N^{30}, N^{01}$ and N^{11} with the ordering $N^{30} \sim N^{11} \sim \epsilon N^{20} \sim \epsilon N^{01} \sim \epsilon \phi$, with ϵ the small expansion parameter

$$\epsilon \sim \frac{1}{\nu} \sim \gamma, \quad (5.1)$$

so that the particle mean-free path $\lambda_{mfp} = v_{th}/\nu_{ei}$ is small compared with typical wavelengths of the perturbed quantities, i.e., $k\lambda_{mfp} \ll 1$. Higher order moments are considered to be $O(\epsilon^2\phi)$. Charge neutrality is kept up to second order, i.e.,

$$\alpha_D \sim \epsilon^2. \quad (5.2)$$

Using Poisson's equation, we find that density perturbations N^{00} are negligible when compared with electrostatic fluctuations, namely

$$\frac{N^{00}}{\phi} = -\alpha_D \ll 1. \quad (5.3)$$

The moment-hierarchy equation, Eq. (2.19), at $(p, j) = (0, 0)$, shows that $N^{10}/N^{00} \sim \gamma$.

Together with the estimate in Eq. (5.3), this yields

$$\frac{N^{10}}{\phi} \sim \gamma \alpha_D \ll 1 \quad (5.4)$$

Using the moment-hierarchy equation Eq. (2.19) and neglecting second order terms in the parallel $(p, j) = (2, 0)$ and perpendicular $(p, j) = (0, 1)$ temperature equations, we find that

$$i\gamma N^{20} \simeq \sqrt{\frac{3}{2}} N^{30} - i\nu(0.45N^{01} + 0.64N^{20}), \quad (5.5)$$

and

$$i\gamma N^{01} \simeq \frac{N^{11}}{\sqrt{2}} - i\nu(0.32N^{01} + 0.45N^{20}), \quad (5.6)$$

respectively. The same procedure in the $(p, j) = (3, 0)$ and $(p, j) = (1, 1)$ moment equations yields

$$0 \simeq \sqrt{\frac{3}{2}} N^{20} - i\nu(0.15N^{11} + 1.03N^{30}), \quad (5.7)$$

and

$$0 \simeq \frac{N^{01}}{\sqrt{2}} - i\nu(1.09N^{11} + 0.15N^{30}), \quad (5.8)$$

respectively.

As a consequence, the truncated moment-hierarchy equations, Eqs. (5.5)-(5.8), yield the following dispersion relation

$$\gamma^2 + 1.96\gamma \left(\frac{1}{\nu} + 0.49\nu \right) + \frac{0.69}{\nu^2} + 1.4 \times 10^{-5}\nu^2 + 0.88 \simeq 0 \quad (5.9)$$

that up to second order in ϵ yields the solutions $\gamma \simeq -0.96\nu - 1.04/\nu$ and $\gamma \simeq -0.92/\nu$. The least damped solution, which is the one consistent with the ordering $\gamma \sim 1/\nu$ in Eq. (5.1), when applied to the $\nu = 5$ case of Fig. 7, leads to $\gamma \simeq -0.18$, which has a relative difference of 11% with respect to the $\gamma = -0.202$ value obtained numerically.

We note that, with the same ordering above, a purely damped solution can also be obtained from the one-dimensional linearized Braginskii equations (Braginskii 1965). In this limit, in fact, the following linearized electron temperature equation is found

$$n_0 \frac{3}{2} \frac{\partial T_e}{\partial t} + \nabla_z \left(-\chi_{\parallel}^e \nabla_z T_e \right) \simeq 0 \quad (5.10)$$

where $\chi_{\parallel}^e = 3.2n_0 T_e / (m_e \nu k v_{th})$, with the Joule heating term proportional to m_e/m_i neglected. Equation (5.10) yields the electron Braginskii entropy mode $\gamma \simeq -1.1/\nu$, a value that is close to the estimate above based on the truncated moment-hierarchy equation.

Finally, we remark that a purely damped mode is only observed in the temporal evolution of N^{00} for values of $\nu \gtrsim 1$, while for $\nu \lesssim 1$ a transition from damped oscillations to a purely damped behaviour is not seen to occur for the range of values of α_D considered here even at later times. The value of ν where a transition from collisional Landau damping to a purely damped entropy mode occurs after an initial transient is visible in the time evolution of N^{00} can be estimated by balancing the damping rate of the collisional damping of EPW with the damping rate of entropy modes. Estimating the former as $\gamma \simeq -0.03 - 0.26\nu$ from Fig. 6, and the latter as $\gamma \simeq -0.92/\nu$, the collision frequency at which the transition occurs is therefore estimated to be $\nu \simeq 1.8$, in agreement with the numerical results.

6. Eigenvalue Spectrum

We now compute the eigenmode spectra of EPW, and highlight the differences between the spectra of the full Coulomb, electron-ion, and Lenard-Bernstein operators using a Hermite-Laguerre decomposition, and the electron-ion operator using a Legendre polynomial decomposition. We note that subdominant and stable modes can be nonlinearly excited to finite amplitude (Terry *et al.* 2006; Hatch *et al.* 2011; Pueschel *et al.* 2016; Hatch *et al.* 2016) and have a major role in nonlinear energy dissipation and turbulence saturation, affecting structure formation, as well as heat and particle transport. We note that both the Lenard-Bernstein and the Dougherty collision operators are seen to yield similar eigenmode spectra. Therefore, we do not consider the Dougherty operator for this analysis. To compute the Hermite-Laguerre EPW eigenmode spectrum, the moment-hierarchy equation, Eq. (2.19), is truncated at a maximum index (P, J) , Fourier transformed in time, and the resulting eigenvalue problem solved numerically, yielding the spectrum of solutions at arbitrary collisionality. In matrix form, this yields

$$\mathbf{A}N = (\omega + i\gamma)N, \quad (6.1)$$

where $N = [N^{00} N^{01} \dots N^{0J} N^{10} N^{11} \dots N^{pj}]$ is the moment vector and \mathbf{A} the $(P+1)(J+1) \times (P+1)(J+1)$ matrix of moment-hierarchy coefficients of elements A_n^m with m and n the row and column, respectively

$$A_{p'J+j'}^{pJ+j} = \sqrt{\frac{p+1}{2}} \delta_{p+1,p'} \delta_{j,j'} + \sqrt{\frac{p}{2}} \delta_{p-1,p'} \delta_{j,j'} + \frac{\delta_{p,1} \delta_{j,0}}{\sqrt{2}} \frac{\delta_{p',0} \delta_{j',0}}{\alpha_D} + iC_{p'J+j'}^{pJ+j}, \quad (6.2)$$

which can be written in matrix form as

$$\mathbf{A} = \begin{bmatrix} 0 & 0 & \dots & 1/\sqrt{2} & 0 & \dots \\ 0 & iC_{01}^{01} & \dots & iC_{10}^{01} & 1/\sqrt{2} + iC_{11}^{01} & \dots \\ \vdots & \vdots & \dots & \vdots & \vdots & \dots \\ (1 + 1/\alpha_D)/\sqrt{2} & iC_{01}^{10} & \dots & iC_{10}^{10} & iC_{11}^{10} & \dots \\ 0 & 1\sqrt{2} + C_{01}^{11} & \dots & iC_{10}^{11} & iC_{11}^{11} & \dots \\ \vdots & \vdots & \dots & \vdots & \vdots & \dots \end{bmatrix}. \quad (6.3)$$

In Eqs. (6.2) and (6.3), we have defined the collisional coefficients C_{st}^{pj} in terms of the collisional moments C^{pj} as $C^{pj} = \sum_{p',j'} C_{p'j'}^{pj} N^{p'j'}$ and $C_{p'J+j'}^{pJ+j} = C_{p'j'}^{pj}$. The spectrum of γ and ω is then found by computing the eigenvalues of the matrix \mathbf{A} .

The resulting eigenvalue spectrum for the Coulomb collision case is shown in Fig. 8 for $\nu = 0.1$ (a) and $\nu = 1$ (b), with $\alpha_D = 0.09$ and $(P, J) = (18, 2)$, together with the corresponding collisionless Landau root (red marker), i.e., the least damped solution of Eq. (3.4). The resulting collisional spectrum is discrete, contrary to the continuous collisionless Van-Kampen spectrum, as noted in previous studies of weakly collisional plasma systems (Ng *et al.* 1999; Bratanov *et al.* 2013). Figure 8 shows that the damping rate of the Coulomb eigenmodes decreases with the corresponding frequency, which is possibly related to the fact that the collisional drag force decreases with the particle velocity in the Coulomb collision operator. We also note that the least damped Coulomb eigenvalue in Fig. 8 is not the one closest to the Landau collisionless solution, as there are modes with higher oscillation frequency ω that are less damped than the collisionless damping rate. These eigenvalue solutions, however, are related to eigenvectors that mainly involve moments N^{pj} with large values of p and j , and have therefore a negligible contribution to the initial damping of N^{00} and ϕ .

Finally, the Coulomb eigenmode spectrum in Fig. 8 includes modes with vanishing

frequency and damping that increases with ν . These modes correspond therefore to purely damped modes with a damping rate that at low collisionalities can be comparable to the collisionless Landau one. These zero-frequency solutions have also been previously observed in the analysis of linear EPW when pitch-angle scattering effects are included (Epperlein *et al.* 1992; Banks *et al.* 2016), and correspond to the entropy mode studied in Section 5.

As an aside, we note that when the moment-hierarchy equation, Eq. (2.19), is truncated at a higher P , i.e., using a higher number of Hermite polynomials, the number of eigenmodes with high frequency and small damping rate increases. On the other hand, when the number of Laguerre polynomials, hence J , is increased, the eigenmode spectrum present and increasing number of modes with similar frequencies but increasingly higher damping rates. However, as shown by Fig. 3, the damping rates γ closest to the collisionless solution have negligible variation when P and J are increased (for $P \geq 18$ and $J \geq 0$ the variation is smaller than 3%).

The eigenmode spectra using a Lenard-Bernstein collision operator are also shown in Fig. 8 for $\nu = 0.1$ (c) and $\nu = 1$ (d), with $\alpha_D = 0.09$ and $(P, J) = (18, 2)$. A clear difference is seen between the eigenmode spectra of the Coulomb and Lenard-Bernstein operators. Contrary to the Coulomb case, the damping rate of the EPW modes increases with the frequency ω when a Lenard-Bernstein collision operator is used. Also, contrary to the Coulomb case, the Lenard-Bernstein root closest to the Landau collisionless root is the least damped one, as also noted in previous weakly-collisional studies of EPW (Bratanov *et al.* 2013).

Finally, the eigenvalue spectrum using the electron-ion Coulomb operator introduced in Eq. (2.36) is shown in Fig. 8 for $\nu = 0.1$ (e) and $\nu = 1$ (f). The spectrum is qualitatively similar to the Coulomb one, with high frequency modes being less damped than modes with smaller oscillation frequency. As for the Coulomb collision operator, such frequency dependence may be due to the dependence of the drag force on the particle velocity. Indeed, the electron-ion collision operator contains a drag force that decreases with the particle velocity, similarly to the Coulomb operator.

We now estimate the frequency ω of the modes in Fig. 8 with a damping rate γ different than the ones closest to the collisionless roots, by noting that the values of ω in Fig. 8 are seen to be weakly dependent on ν , α_D , and the collision operator for the range of values used. We therefore solve the moment-hierarchy equation, Eq. (2.19), in the $\phi = 0$ limit, which effectively neglects the roots related to EPW. Furthermore, in order to retrieve purely oscillatory solutions, the collisional damping terms C^{pj} in Eq. (2.19) are neglected. The time Fourier-transformed moment-hierarchy equation in the $\phi = C^{pj} = 0$ limit reads

$$\omega N^{pj} = \sqrt{\frac{p+1}{2}} N^{p+1j} + \sqrt{\frac{p}{2}} N^{p-1j}. \quad (6.4)$$

We recognize in Eq. (6.4) the recursion relation for the Hermite polynomials

$$N^{pj} = \frac{H_p(\omega)}{\sqrt{2^p p!}}. \quad (6.5)$$

The roots ω can be found by applying the truncation condition in Eq. (4.1) to the solution in Eq. (6.5), yielding

$$H_{P+1}(\omega) = 0. \quad (6.6)$$

The solutions ω in Eq. (6.6) are purely real, yielding frequencies that closely follow the ones observed in the eigenvalue spectra (red vertical lines in Fig. 8).

Finally, we present two tests to assess the validity of the results in Fig. 8, first for

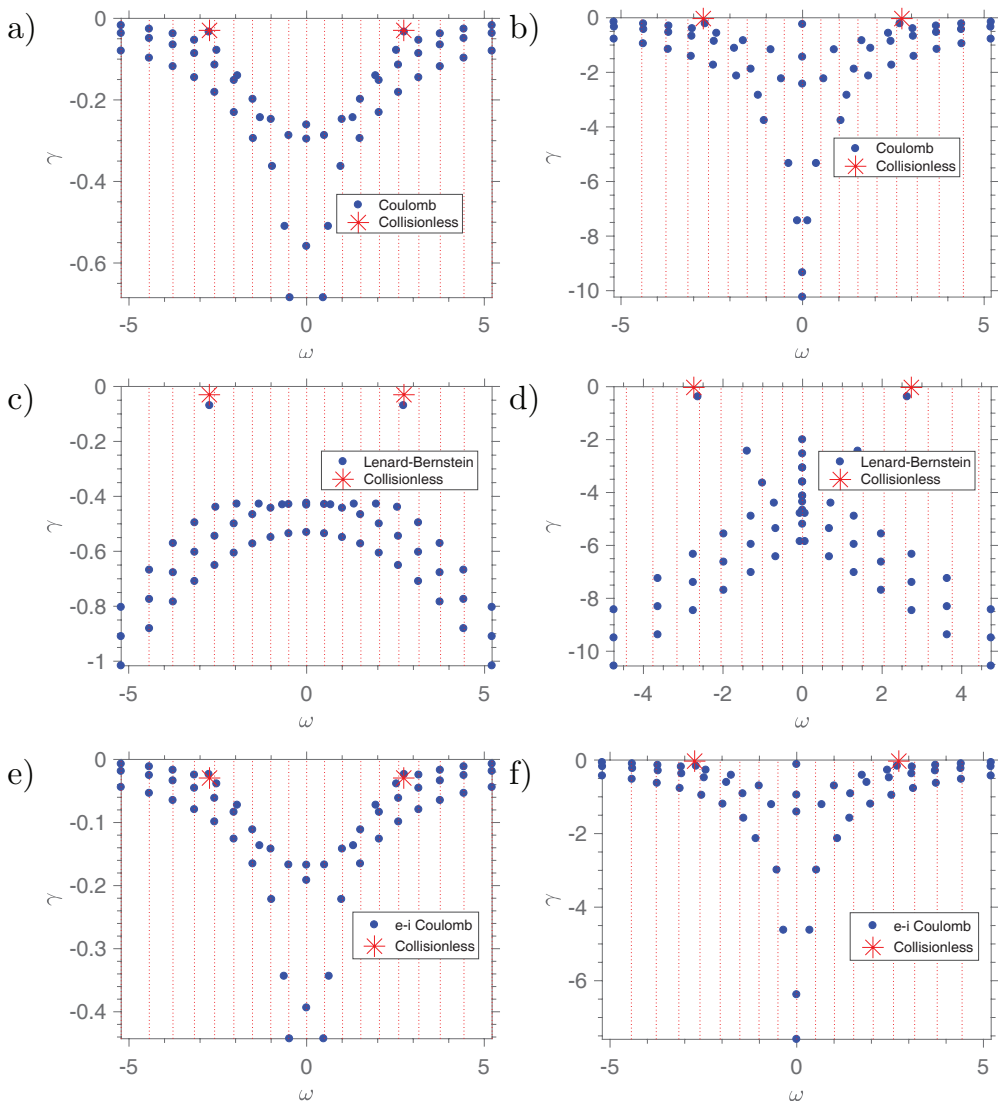


FIGURE 8. Complete eigenvalue spectrum of the truncated moment-hierarchy equation with $\alpha_D = 0.09$ and $(P, J) = (18, 2)$ [yielding $(P + 1)(J + 1) = 57$ eigenvalues], using the full-Coulomb collision operator (top), the Lenard-Bernstein operator (middle), and the electron-ion Coulomb operator only (bottom), with $\nu = 0.1$ (left) and $\nu = 1$ (right). The collisionless least damped solution is shown as a red marker, and the red vertical lines are the solutions of Eq. (6.6).

the Lenard-Bernstein case and then for the electron-ion case. Focusing on the Lenard-Bernstein spectrum, we derive a polynomial in γ whose roots closely follow the modes in Fig. 8 (c) and (d) that appear with damping rates larger than the ones of the two least damped roots. Fourier transforming the Boltzmann equation, Eq. (2.10), in time and in velocity-space similarly to Ng *et al.* (2004), with $C(f)$ the Lenard-Bernstein collision operator, the following differential equation for $g(s) = \int_{-\infty}^{\infty} \exp(isv_z - \gamma t + i\omega t) f_M \delta f_k dv_z dt$ is obtained

$$g(s) \left(\gamma + i\omega + \frac{\nu}{2} s^2 \right) + (1 + \nu s) \frac{dg(s)}{ds} = -s \frac{\sqrt{\pi}}{2\alpha_D} e^{-\frac{s^2}{4}} g(0). \quad (6.7)$$

We solve Eq. (6.7) neglecting the coupling with the electrostatic potential ϕ by setting $\alpha_D \gg 1$ (or, equivalently, setting $\phi = 0$ in the Boltzmann equation), and define $\lambda = \nu^{-2}/2$ and $\Gamma = \sqrt{2\lambda}(\gamma + i\omega) - \lambda$, yielding

$$g(s) = g(0) \left(1 + \frac{s}{2\lambda}\right)^\Gamma e^{-\frac{s^2}{4} + s\lambda}. \quad (6.8)$$

Similarly, Fourier transforming the Hermite-Laguerre expansion of $\langle \delta f_k \rangle$ in velocity-space, we obtain

$$g(s) = \sum_{p=0}^{\infty} \frac{i^p N^{p0}}{\sqrt{2^{p+1} p!}} s^p e^{-\frac{s^2}{4}}. \quad (6.9)$$

Equating the two expressions above, we find

$$N^{p0} = N^{00} (-i)^p \sqrt{\frac{2^{p+1}}{p!}} \frac{d^p}{ds^p} \left[e^{s\lambda} \left(1 + \frac{s}{2\lambda}\right)^\Gamma \right]_{s=0}. \quad (6.10)$$

Therefore, the truncation condition in Eq. (4.1) in the $\phi = 0$ limit is equivalent to imposing

$$\frac{d^P}{ds^P} \left[e^{s\lambda} \left(1 + \frac{s}{2\lambda}\right)^\Gamma \right]_{s=0} = 0. \quad (6.11)$$

Finally, we can rewrite Eq. (6.11) as a polynomial in $\gamma + i\omega$

$$\sum_{t=0}^P a_{Pt}(\lambda) (\gamma + i\omega)^t = 0, \quad (6.12)$$

with

$$a_{pt}(\lambda) = \sum_{l=t}^P \sum_{n=l}^P \binom{p}{n} \binom{l}{t} s(n, l) \lambda^{p+l-n-t/2} (-1)^{l-t} 2^{t/2}, \quad (6.13)$$

where $s(n, l)$ are the Stirling numbers of the first kind (Moser & Wyman 1958; Qi 2014). As shown in Fig. 9, the polynomial expression in Eq. (6.12) closely reproduces the eigenvalue spectrum observed in Fig. 8 (c) and (d). Therefore, although the coupling of the electron distribution function with ϕ is crucial to reproduce the EPW roots, additional modes in the eigenmode spectrum are related to solutions decoupled from the electrostatic potential ϕ , subject to the truncation condition of the Hermite-Laguerre series, Eq. (4.1), with frequencies similar to the ones of Eq. (6.6).

As a second test, to assess the validity of the eigenmode spectrum found with an electron-ion collision operator in Fig. 8, we solve the Boltzmann equation using a different set of basis functions, namely expanding $\langle \delta f_k \rangle$ in Legendre polynomials, Eq. (2.40), and solving the resulting moment-hierarchy equation, Eq. (2.40), numerically. In this case, the expansion of $\langle \delta f_k \rangle$ in Eq. (2.39) is truncated at $l_{max} = L$ by setting $a_{L+1} = 0$. The velocity v is discretized over an interval $[0, v_{max}]$ with an equidistant mesh made of n_v points, and the integral estimated with a composite trapezoidal rule. The resulting spectrum is shown in Fig. 10. When compared with the Hermite-Laguerre spectrum in Fig. 8 (e) and (f), the two spectra look qualitatively similar, confirming the validity of the Hermite-Laguerre approach. However, a higher number of small-damped low-frequency solutions is observed when a Legendre decomposition is used. The appearance of small-damped non-physical eigenmodes when using a finite-difference discretization in v was also noted by Bratanov *et al.* (2013), leading to the conclusion that, in general, a Hermite discretization of the distribution function is in fact superior to a finite difference one. Furthermore, for the values of $\nu = 0.02$ and $\alpha_D = 0.09$ where the Hermite-Laguerre

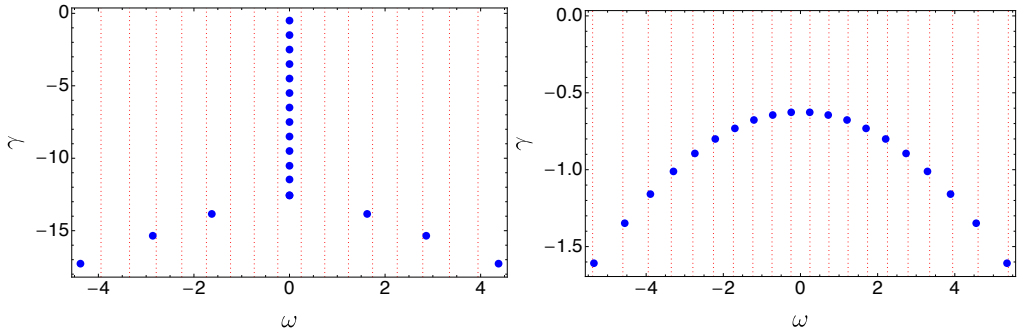


FIGURE 9. Blue dots: roots of the polynomial in Eq. (6.12), which corresponds to the solution of the Boltzmann equation with a Lenard-Bernstein collision operator where the distribution function is approximated by a truncated Hermite expansion, for $\lambda = 50$ (left) and $\lambda = 0.5$ (right) (corresponding to $\nu = 0.1$ and 1 , respectively) at $P = 20$. Red vertical lines: solutions of Eq. (6.6).

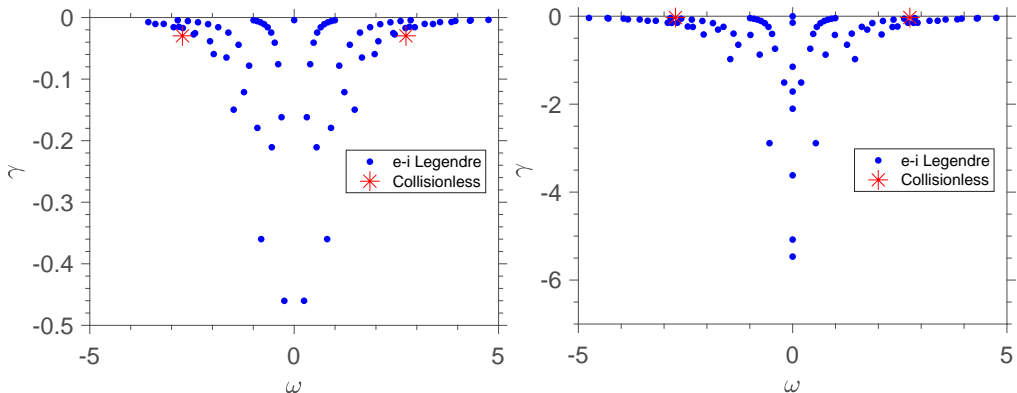


FIGURE 10. Eigenvalue spectrum of the truncated moment-hierarchy equation using an electron-ion Coulomb collision operator for $\nu = 0.1$ (left) and $\nu = 1.0$ (right) with $\alpha_D = 0.09$, $n_v = 12$ and $L = 7$, with a Legendre decomposition. The collisionless solution is shown with a red marker.

formulation with $(P + 1)(J + 1) = 19 \times 3 = 57$ polynomials is seen to converge to the collisionless Landau solution in Fig. 6 with a relative difference of $\sim 16\%$, when using a Legendre decomposition, a total of $n_v \times L \simeq 100$ equations is needed to yield a similar accuracy on γ .

7. Conclusion

In this work, for the first time, the effect of full Coulomb collisions on electron-plasma waves is studied by taking into account both electron-electron and electron-ion collisions in their exact form. The analysis is performed using an expansion of the distribution function and the Coulomb collision operator in a Hermite-Laguerre polynomial basis. The proposed framework is particularly efficient, as the number of polynomials needed in order to obtain convergence is low enough to allow multiple scans to be performed, particularly a comparison between several collision operators at arbitrary collisionalities. While the use of electron-ion collisions alone is seen to slightly decrease the damping rate with respect to full Coulomb collisions, the damping rate using a Lenard-Bernstein or a Dougherty collision operator is seen to yield deviations up to 50% larger with respect to the Coulomb one. An eigenmode analysis reveals major differences between the

spectrum of full Coulomb and simplified collision operators. The eigenspectrum reveals the presence of purely damped modes that, as shown, correspond to the entropy mode. In the collisional limit, the entropy mode is observed to set the long time behavior of the system with a damping rate smaller than the Landau damping one. We show that this mode needs a full-Coulomb collision operator for its proper description. Furthermore, we find an analytical dispersion relation for the entropy mode that accurately reproduces the numerical results.

8. Acknowledgements

This work has been carried out within the framework of the EUROfusion Consortium and has received funding from the Euratom research and training programme 2014-2018 and 2019 - 2020 under grant agreement No 633053, and from Portuguese FCT - Fundação para a Ciência e Tecnologia, under grant PD/BD/105979/2014, carried out as part of the training in the framework of the Advanced Program in Plasma Science and Engineering (APPLAuSE, sponsored by FCT under grant No. PD/00505/2012) at Instituto Superior Técnico (IST). S.G. acknowledges financial support from Fusenet. N.F.L. was partially funded by US Department of Energy Grant no. DE-FG02-91ER54109. This work was supported in part by the Swiss National Science Foundation. The views and opinions expressed herein do not necessarily reflect those of the European Commission.

REFERENCES

- BANKS, J. W., BRUNNER, S., BERGER, R. L., ARRIGHI, W. J. & TRAN, T. M. 2017 Collisional damping rates for electron plasma waves reassessed. *Physical Review E* **96** (4), 043208.
- BANKS, J. W., BRUNNER, S., BERGER, R. L. & TRAN, T. M. 2016 Vlasov simulations of electron-ion collision effects on damping of electron plasma waves. *Physics of Plasmas* **23** (3), 032108.
- BELLI, E. A. & CANDY, J. 2008 Kinetic calculation of neoclassical transport including self-consistent electron and impurity dynamics. *Plasma Physics and Controlled Fusion* **50** (9), 095010.
- BOHM, D. & GROSS, E. P. 1949 Theory of plasma oscillations. A. Origin of medium-like behavior. *Physical Review* **75** (12), 1851.
- BRAGINSKII, S. I. 1965 Transport processes in a plasma. *Reviews of Plasma Physics* **1**, 205.
- BRANTOV, A. V., BYCHENKOV, V. YU. & ROZMUS, W. 2012 Electrostatic response of a two-component plasma with coulomb collisions. *Physical Review Letters* **108** (20), 205001.
- BRATANOV, V., JENKO, F., HATCH, D. & BRUNNER, S. 2013 Aspects of linear Landau damping in discretized systems. *Physics of Plasmas* **20** (2), 022108.
- BRUNNER, S. & VALEO, E. J. 2004 Trapped-particle instability leading to bursting in stimulated Raman scattering simulations. *Physical Review Letters* **93** (14), 145003.
- CALLEN, J. D. & KISSICK, M. W. 1997 Evidence and concepts for non-local transport. *Plasma Physics and Controlled Fusion* **39** (39), 173.
- DAWSON, J. 1961 On Landau damping. *Physics of Fluids* **4** (7), 869.
- DOUGHERTY, J. P. 1964 Model Fokker-Planck Equation for a Plasma and Its Solution. *Physics of Fluids* **7** (11), 1788.
- EPERLEIN, E. M. 1994 Effect of electron collisions on ion-acoustic waves and heat flow. *Physics of Plasmas* **1** (1), 109.
- EPERLEIN, E. M., SHORT, R. W. & SIMON, A. 1992 Damping of ion-acoustic waves in the presence of electron-ion collisions. *Physical Review Letters* **69** (12), 1765.
- GAUTSCHI, WALTER 1970 Efficient Computation of the Complex Error Function. *SIAM Journal on Numerical Analysis* **7** (1), 187.
- GRANDGIRARD, V., ABITEBOUL, J., BIGOT, J., CARTIER-MICHAUD, T., CROUSEILLES, N., DIF-PRADALIER, G., EHRLACHER, CH, ESTEVE, D., GARBET, X., GHENDRIH, PH, LATU, G., MEHRENBERGER, M., NORSCINI, C., PASSERON, CH, ROZAR, F., SARAZIN, Y.,

- SONNENDRÜCKER, E., STRUGAREK, A. & ZARZOSO, D. 2016 A 5D gyrokinetic full-f global semi-Lagrangian code for flux-driven ion turbulence simulations. *Computer Physics Communications* **207**, 35.
- HAMMETT, G. W., BEER, M. A., DORLAND, W. D., COWLEY, S. C. & SMITH, S. A. 1993 Developments in the gyrofluid approach to tokamak turbulence simulations. *Plasma Physics and Controlled Fusion* **35** (8), 973.
- HAMMETT, G. W., DORLAND, W. & PERKINS, F. W. 1992 Fluid models of phase mixing, Landau damping, and nonlinear gyrokinetic dynamics. *Physics of Fluids B: Plasma Physics* **4** (7), 2052.
- HAMMETT, G. W. & PERKINS, F. W. 1990 Fluid moment models for Landau damping with application to the ion-temperature-gradient instability. *Physical Review Letters* **64** (25), 3019.
- HATCH, D. R., JENKO, F., NAVARRO, A. B., BRATANOV, V., TERRY, P. W. & PUESCHEL, M. J. 2016 Linear signatures in nonlinear gyrokinetics: interpreting turbulence with pseudospectra. *New Journal of Physics* **18** (7), 075018.
- HATCH, D. R., TERRY, P. W., JENKO, F., MERZ, F. & NEVINS, W. M. 2011 Saturation of gyrokinetic turbulence through damped eigenmodes. *Physical Review Letters* **106** (11), 115003.
- HELANDER, P. & SIGMAR, D. 2005 *Collisional transport in magnetized plasmas*. Cambridge: Cambridge University Press.
- HUNANA, P., ZANK, G. P., LAURENZA, M., TENERANI, A., WEBB, G. M., GOLDSTEIN, M. L., VELLI, M. & ADHIKARI, L. 2018 New closures for more precise modeling of Landau damping in the fluid framework. *Physical Review Letters* **121** (13), 135101.
- JACKSON, J. D. 1960 Longitudinal plasma oscillations. *Journal of Nuclear Energy. Part C* **1** (4), 171.
- JI, J.-Y. & HELD, E. D. 2006 Exact linearized Coulomb collision operator in the moment expansion. *Physics of Plasmas* **13** (10), 102103.
- JI, J.-Y. & HELD, E. D. 2010 Analytical solution of the kinetic equation for a uniform plasma in a magnetic field. *Physical Review E* **82** (1), 016401.
- JORDANOVA, V. K., KISTLER, L. M., KOZYRA, J. U., KHAZANOV, G. V. & NAGY, A. F. 1996 Collisional losses of ring current ions. *Journal of Geophysical Research* **101** (A1), 111.
- JORGE, R., RICCI, P. & LOUREIRO, N. F. 2017 A drift-kinetic analytical model for scrape-off layer plasma dynamics at arbitrary collisionality. *Journal of Plasma Physics* **83** (6), 905830606.
- JORGE, R., RICCI, P. & LOUREIRO, N. F. 2018 Theory of the Drift-Wave Instability at Arbitrary Collisionality. *Physical Review Letters* **121** (16), 165001.
- JOSEPH, I. & DIMITS, A. M. 2016 Connecting Collisionless Landau Fluid Closures to Collisional Plasma Physics Models. *Contributions to Plasma Physics* **56** (6), 504.
- LANDAU, L. D. 1946 On the Vibrations of the Electronic Plasma. *Journal of Physics U.S.S.R.* **10** (1), 25.
- LANDREMAN, M. & ERNST, D. R. 2013 New velocity-space discretization for continuum kinetic calculations and Fokker-Planck collisions. *Journal of Computational Physics* **243** (15), 130.
- LENARD, A. & BERNSTEIN, I. B. 1958 Plasma oscillations with diffusion in velocity space. *Physical Review* **112** (5), 1456.
- LIEBERMAN, M. A. & LICHTENBERG, A. J. 2005 *Principles of Plasma Discharges and Materials Processing*. Wiley.
- LINDL, J. D., AMENDT, P., BERGER, R. L., GLENDINNING, S. G., GLENZER, S. H., HAAN, STEVEN W., KAUFFMAN, R. L., LANDEN, O. L. & SUTER, L. J. 2004 The physics basis for ignition using indirect-drive targets on the National Ignition Facility. *Physics of Plasmas* **11** (2), 339.
- LOUREIRO, N. F., DORLAND, W., FAZENDEIRO, L., KANEKAR, A., MALLET, A., VILELAS, M. S. & ZOCCO, A. 2016 Viriato: A Fourier-Hermite spectral code for strongly magnetized fluid-kinetic plasma dynamics. *Computer Physics Communications* **206**, 45.
- MALMBERG, J. H. & WHARTON, C. B. 1966 Dispersion of Electron Plasma Waves. *Physical Review Letters* **17** (4), 175.

- MANDELL, N. R., DORLAND, W. & LANDREMAN, M. 2018 Laguerre-Hermite pseudo-spectral velocity formulation of gyrokinetics. *Journal of Plasma Physics* **84** (01), 905840108.
- MORALES, G. J. & O'NEIL, T. M. 1972 Nonlinear frequency shift of an electron plasma wave. *Physical Review Letters* **28** (7), 417.
- MOSER, L. & WYMAN, M. 1958 Asymptotic development of the stirling numbers of the first kind. *Journal of the London Mathematical Society* **s1** (2), 133.
- MOUHOT, C. & VILLANI, C. 2011 On Landau damping. *Acta Mathematica* **207** (1), 29.
- NAKATA, M., HONDA, M., YOSHIDA, M., URANO, H., NUNAMI, M., MAEYAMA, S., WATANABE, T. & SUGAMA, H. 2016 Validation studies of gyrokinetic ITG and TEM turbulence simulations in a JT-60U tokamak using multiple flux matching. *Nuclear Fusion* **56** (8), 086010.
- NG, C. S., BHATTACHARJEE, A. & SKIFF, F. 1999 Kinetic eigenmodes and discrete spectrum of plasma oscillations in a weakly collisional plasma. *Physical Review Letters* **83** (10), 1974.
- NG, C. S., BHATTACHARJEE, A. & SKIFF, F. 2004 Complete Spectrum of Kinetic Eigenmodes for Plasma Oscillations in a Weakly Collisional Plasma. *Physical Review Letters* **92** (6), 065002.
- O'NEIL, T. M. & ROSTOKER, N. 1965 Triplet Correlation for a Plasma. *Physics of Fluids* **8** (6), 1109.
- OPHER, M., MORALES, G. J. & LEBOEUF, J. N. 2002 Krook collisional models of the kinetic susceptibility of plasmas. *Physical Review E - Statistical Physics, Plasmas, Fluids, and Related Interdisciplinary Topics* **66** (1), 016407.
- PAN, Q., TOLD, D., SHI, E., HAMMETT, G. W. & JENKO, F. 2018 Full-f version of GENE for turbulence in open-field-line systems. *Physics of Plasmas* **25** (6), 062303.
- PUESCHEL, M. J., FABER, B. J., CITRIN, J., HEGNA, C. C., TERRY, P. W. & HATCH, D. R. 2016 Stellarator Turbulence: Subdominant Eigenmodes and Quasilinear Modeling. *Physical Review Letters* **116** (8), 085001.
- QI, F. 2014 Explicit formulas for computing Bernoulli numbers of the second kind and stirling numbers of the first kind. *Filomat* **28** (2), 319.
- SCHEKOCIHIN, A. A., PARKER, J. T., HIGHCOCK, E. G., DELLAR, P. J., DORLAND, W. & HAMMETT, G. W. 2016 Phase mixing versus nonlinear advection in drift-kinetic plasma turbulence. *Journal of Plasma Physics* **82** (2), 905820212.
- SCOTT, B. D. 2007 Tokamak edge turbulence: Background theory and computation. *Plasma Physics and Controlled Fusion* **49** (7), S25.
- SHAMPINE, L. F. 2002 Solving $0 = F(t, y(t), y'(t))$ in matlab. *Journal of Numerical Mathematics* **10** (4), 291.
- SHI, E. L., HAMMETT, G. W., STOLTZFUS-DUECK, T. & HAKIM, A. 2017 Gyrokinetic continuum simulation of turbulence in a straight open-field-line plasma. *Journal of Plasma Physics* **83** (03), 905830304.
- TERRY, P. W., BAVER, D. A. & GUPTA, S. 2006 Role of stable eigenmodes in saturated local plasma turbulence. *Physics of Plasmas* **13** (2), 022307.
- TRACY, M. D., WILLIAMS, E. A., ESTABROOK, K. G., DE GROOT, J. S. & CAMERON, S. M. 1993 Eigenvalue solution for the ion-collisional effects on ion-acoustic and entropy waves. *Physics of Fluids B* **5** (5), 1430.
- WAX, N. 1954 *Selected Papers on Noise and Stochastic Processes*. New York, United States: Dover Publications.
- WINJUM, B. J., BERGER, R. L., CHAPMAN, T., BANKS, J. W. & BRUNNER, S. 2013 Kinetic simulations of the self-focusing and dissipation of finite-width electron plasma waves. *Physical Review Letters* **111** (10), 105002.
- ZAKHAROV, V. E. 1972 Collapse of Langmuir Waves. *Soviet Physics JETP* **35** (5), 908.
- ZHENG, J. & YU, C. X. 2000 Ion-collisional effects on ion-acoustic waves: an eigenvalue technique via moment expansion. *Plasma Physics and Controlled Fusion* **42** (4), 435.
- ZOCCO, A., LOUREIRO, N. F., DICKINSON, D., NUMATA, R. & ROACH, C. M. 2015 Kinetic microtearing modes and reconnecting modes in strongly magnetised slab plasmas. *Plasma Physics and Controlled Fusion* **57** (6), 065008.
- ZOCCO, A. & SCHEKOCIHIN, A. A. 2011 Reduced fluid-kinetic equations for low-frequency dynamics, magnetic reconnection, and electron heating in low-beta plasmas. *Physics of Plasmas* **18** (10), 102309.